Automatic Accuracy Assessment of Ultrasound Elastography Using Correlation Profile and Prior Information of Displacement Continuity

M. Ghasemi Amidabadi, M. Omair Ahmad, *Fellow, IEEE*, and H. Rivaz, *Member, IEEE*

***Abstract*—Calculation of the Normalized Cross Correlation (NCC) at the estimated displacement has been usually the only way to assess the accuracy of Time-Delay Estimation (TDE) in elastography in recent years. However, a method is proposed in [1] which takes advantage of using *NCC profile* with 7 valuable features and also looks at accuracy assessment in a supervised approach. In this paper, we build on our previous work by utilizing continuity features in axial and lateral directions as useful information. We show that these features improve the sensitivity and specificity of the classifier. After extracting the continuity features in addition to features proposed in our previous work, we train a linear Support Vector Machine (SVM) on three *in-vivo* data sets to show the significant improvement of utilizing the proposed features.**

***Index Terms*—Accuracy Assessment, Ultrasound Imaging, Ultrasound Elastography, Supervised Quality Assessment**

I. Introduction

Ultrasound elastography is well studied in literature as an imaging technique to measure mechanical properties of the tissue, specially those are related to the elastic modulus [2], [3]. To this end, several elastography methods are established to obtain deformation field between two frames of ultrasound Radio-Frequency (RF) data, a problem also referred to as Time-Delay Estimates (TDE) [4]. Obtaining accurate TDE is a challenging due to large signal decorrelation noise which can adversly affect accuracy of elastography algorithms. Accuracy assessment of TDE can be used to mask out erroneous areas of strain images, improve quality of strain images by exploiting weighted averaging of elasticity images [3], [5], and to speed up training duration of sonographers to acquire images of higher quality instead of relying on individual's skills.

Reliable quality assessment of TDE plays an important role in widespread use of ultrasound elastography. Early work found lower bounds for the variance of the displacement estimate errors [6], [7], [8], [9]. Although this approach tries to find a closed-from expression for any unbiased TDE method based on TDE parameters and ultrasound system configuration, it can not provide accuracy of TDE. General performance metrics such as signal-to-noise ratio (SNR) and contrast-to-noise ratio (CNR) of the strain images were therefore proposed to overcome this pitfall of the lower bound error analysis. These values are usually measured as a function of axial strain and are called strain filter [10], [11], [12], [13], [14]. Two disadvantages can be considered in using SNR and CNR as measures of quality assessment. First, they are measured in a small and homogenous regions in strain image which are not always available in real tissue. Second, these values are not calculated directly from TDE. Instead they are obtained through derivative of TDE that would definitely depend on derivative operator.

A common method to assess the accuracy of TDE is by using Normalized Cross Correlation (NCC). NCC is calculated between two windows in corresponding RF frames to provide a quantified insight regarding accuracy of TDE. In [15], regions in which corresponding NCC values are less than a user-defined threshold are masked out as incorrect areas of the strain image. In [16], [17], [18], precision of the displacement field is linked to the value of NCC, which is later used to wash out the incorrect areas of the strain image. In [19], consistency information of consecutive frames is incorporated as measure to assess the quality of strain images. In [20], a method is introduced which selects a few representative frames from a large pool of axial strain images and assigns each frame a quality indicator and performs a weighted averaging of the strain images based on their NCC values. All of aforementioned methods utilize only the value of the NCC at the estimated displacement. Finally, a method is presented in [1] which uses information of the NCC profile around the estimated time-delay. Seven features are proposed in the method to recognize peak-hoping and jitter error in TDEs. Specifically, Skewness and variance of nine neighboring NCC values are used to distinguish peak-hoping samples and the only NCC value at the estimated displacement in addition to four closest neighboring NCC values which are utilized to find jitter error. After extracting those seven features, a linear SVM model is trained as binary classifier to evaluate the accuracy of TDEs. However, the proposed method does not take into account continuity of TDE in displacement field due to homogeneity properties of the tissue. Although accurate TDE is not available for patient data sets, Dynamic Programming Analytic Minimization (DPAM) [21] has been used in the method to provide ground truth for training the model.

Herein, we extract two additional features in addition to the seven features in [1] to improve the distinguishability of the proposed model on three *in-vivo* data sets. Moreover, a new and accurate elastography method which is called Global Ultrasound Elastography (GLUE) [22] is utilized to get more

This work was supported by grants RGPIN-2015-04136 and RGPIN-06623 from Natural Sciences and Engineering Research Council (NSERC) of Canada. Authors are with the Department of Electrical and Computer Engineering, Concordia University, Montreal, QC, H3G 1M8, Canada. Email: m_hase, omair, hrivaz@ece.concordia.ca

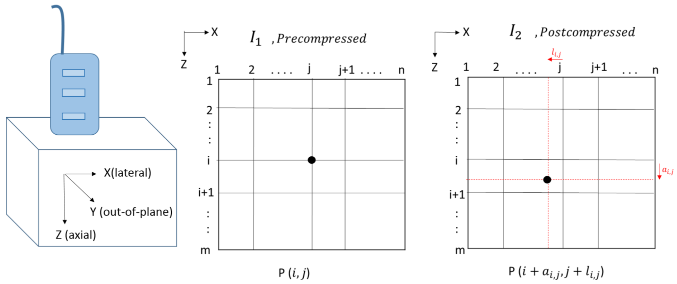

Fig. 1. Displacement between pre-and post compressed images. I_1 and I_2 are pre- and post-compressed images, respectively. Z, X, Y are axial, lateral and out-of-plane directions, respectively. The coordinate system is attached to the ultrasound probe. The sample P (i,j) in I_1 has been moved by ($a_{i,j}$,$l_{i,j}$) in I_2.

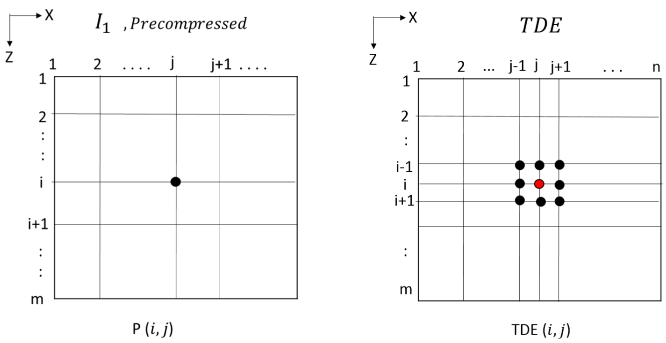

Fig. 2. Pre-compressed image on the left and the corresponding TDE between I_1 and I_2 on the right. For sample P (i,j) in I_1, eight neighboring TDE values are shown as black points on the right image.

accurate TDE values for *in-vivo* data sets in training classifiers. And then, performance of the proposed method is investigated using the aforementioned nine features on all three patients.

II. Methods

Let I_1 and I_2 be pre-and post-compressed images in Fig. 1, and the displacement field obtained by an elastography algorithm corresponds to samples in I_1 and I_2 images. For each sample (i,j) in the pre-compressed image, a and l show axial and lateral displacement values, respectively in Fig. 1. In [1], accuracy of TDE is evaluated in a supervised approach using information of NCC profile and seven valuable features are proposed for training the model.

Continuity (i.e. lack of rupture) in real tissue implies that TDEs should not change significantly in a small region in tissue. Therefore, for each sample (i,j) in I_1, a window of size 3 by 3 is taken into account in displacement field so that variance of those nine TDE values in axial and lateral directions are taken as continuity features according to Fig. 2. This means in a case that peak-hoping sample happens, TDE is estimated far from the correct TDE and these variances will be increased incredibly in which peak-hoping samples will be simply classified as incorrect TDE.

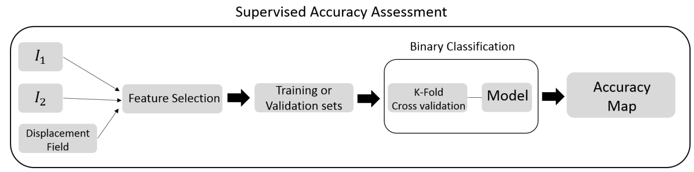

Fig. 3. Flowchart of the proposed method. I_1 and I_2 are pre- and post-compressed images, respectively. Displacement field is available from a displacement estimation algorithm.

A. *Supervised Learning*

In this work, Support Vector Machine (SVM) is trained for the supervised quality assessment of time-delay estimates. SVM is a supervised classification method and is utilized as binary classifier to categorize correct and incorrect estimated time-delays. Therefore, it requires training an testing samples categorized as true and false classes which are formed according to the scheme that is thoroughly described in [1].

B. *Training Sets*

For *in-vivo* data, the ground truth TDE is not available. In [1], a method based on DPAM of a regularized cost function was used. Although the method was accurate enough, we want to show that the proposed scheme would work even in case of using another accurate method in obtaining ground truth of TDE for patient data. Therefore, we utilize the new and more reliable proposed elastography algorithm in [22] to find the correct TDE as ground truth. The method known as Global Ultrasound Elastography (GLUE), finds all TDE values for all RF frames simultaneously by using a non-linear cost function and is optimized in an efficient way. In addition, the quality of strain images are visually checked before using GLUE TDEs to ensure that GLUE is successful in providing accurate displacement fields.

C. *Classification*

The main purpose of this work is to add continuity features to those seven valuable features discussed in [1] to improve the quality of supervised classification. Therefore, for each sample (i,j) in I_1, nine features are calculated to train and validate the proposed model. In Fig. 3, flowchart of the proposed method is shown to better illustrate different stages of the supervised accuracy assessment.

III. Results

This work is implemented in MATLAB and is tested on three clinical data sets. This approach makes use of all samples of I_1 in training and testing. This means that for each sample (i,j) in I_1, windows of size 51 by 1 are considered for calculating the NCC values to obtain seven features discussed in [1] and then variances of corresponding samples in displacement field are calculated. For training, true and false classes are needed. Therefore, true class is formed by using GLUE method and false class is constructed by finding peak-hoping samples and adding an uniform noise to the rest of the samples

TABLE I

CLASSIFICATION ACCURACY USING ONE NCC VALUE, 7 FEATURES, AND 9 FEATURES FOR THREE PATIENT DATA USING SVM CLASSIFIER.

Data set	1-NCC	7-Features	9-Features
Patient data 1	66.7	82.7	84.1
Patient data 2	69.2	83.9	85.2
Patient data 3	81.2	91.5	95.6
Average	72.3	86	88.3

in TDEs in both axial and lateral directions. The uniform noise is in the range of [0.4 0.6] sample in the axial and [-0.1 0.1] sample in the lateral direction meaning that there is always a minimum 0.4 sample error in the axial direction for all samples in false class.

A. In-Vivo Data

The RF data was acquired at Johns Hopkins University using an Antares Siemens (Issaquah, WA) ultrasound machine and A VF10-5 linear array at the center frequency of 6.67 MHz with a sampling rate of 40 MHz. All three *in-vivo* data sets are obtained from ablation therapy of the patients with liver cancer. As mentioned before, the displacement field for all the three patients is calculated utilizing the GLUE method [22].

The overall classification accuracy using one NCC value, seven and nine features are shown in Table 1 for all the three patients. The accuracy is improved by more than 14% on the average by using the seven features and more than 16 % on the average by using the nine features. In first and second patient data, peak-hoping samples in forming the false class involves 2% of all incorrect samples and rest of them are jitter samples. However, we added more peak-hoping samples to the third patient's false class (10% of the false class) to show the power of the two proposed features. Although using the nine features for the third patient is improving the results, it has the disadvantage of requiring a larger training sample (i.e. peak-hoping samples), which comes with increased computational cost. Last but not least, the Receiver Operating Characteristic (ROC) curves for all the three patients are depicted in Fig. 4. The area under the ROC curve is increased from 0.6932 to 0.8965 for patient 1, from 0.7477 to 0.9008 for patient 2 and from 0.8777 to 0.9707 for patient 3 by using the nine features. The improvements achieved by utilizing the information of the NCC profile around the time-delay estimate and locally continuity properties of the displacement field due to continuity of the displacement field.

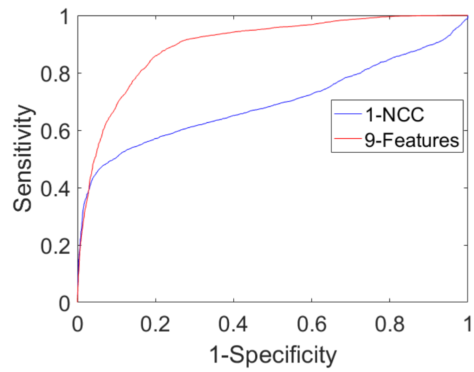

(a) patient 1

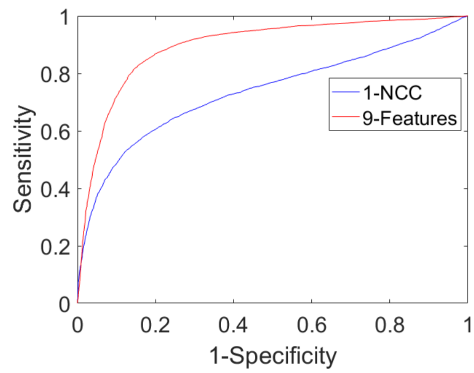

(b) patient 2

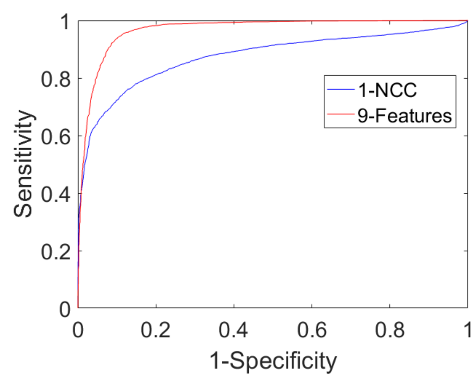

(c) patient 3

Fig. 4. ROC curves for three patients.

B. Accuracy Map in Region of Interest (ROI)

Quantitative validation of the proposed model and features has been done in the previous sections. Herein, the accuracy map of the scheme is visualized for patient 3. The red boxes in Figs. 9 (a) and (b), show tumor region in B-mode ultrasound and strain image, respectively. To visualize the performance of the proposed method, two experiments are performed. First, the displacement field for the tumor region is obtained by GLUE and is visually checked. Therefore, the binary classifier should recognize them as true displacement estimate. In Figs. 9 (c) and (d), results of using one NCC and nine features are shown. Yellow samples indicate correct classified regions and blue samples show incorrect classified samples. Second, all samples in tumor region are peak-hoping or corrupted by noise as jitter samples. Therefore, the proposed method should classify them as incorrect estimates. Figs. 9 (e) and (f) show the result of using the method for using one NCC and nine features values, respectively. Correct and incorrect classifications are indicated in yellow and blue, respectively. The results distinctly demonstrate that using the nine features

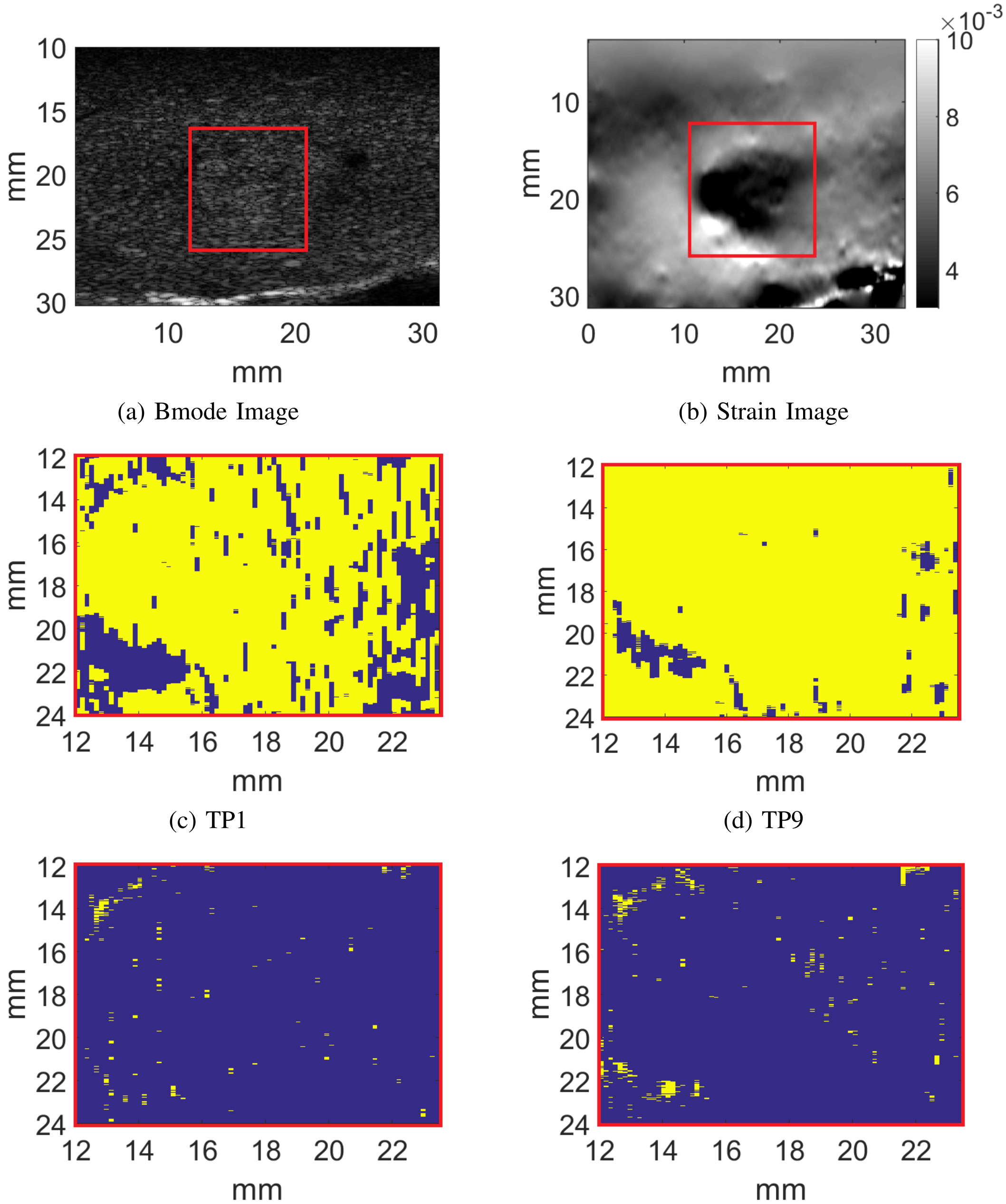

(a) Bmode Image (b) Strain Image

(c) TP1 (d) TP9

(e) FP1 (f) FP9

Fig. 5. Accuracy map in tumor region for patient 3 is shown in red boxes for true and false positive cases.

outperforms utilizing only one NCC value.

IV. Conclusion

A new method for accuracy assessment of TDE in ultrasound elastography is presented using NCC profile and continuity of the tissue displacement field. The approach considers accuracy of TDE at each sample as a binary classification problem meaning that each estimate is labelled as correct or incorrect. Therefore, erroneous areas of the strain image can be masked out to only show correctly estimated regions. This method also reduces dependency of the quality of ultrasound images on skills of sonographers. We used GLUE [22] in this paper for performing TDE. However, any other reliable elastography algorithms is applicable in our proposed method. The performance of the proposed method is validated on three patient data sets. Although training the SVM model is computationally expensive, it is performed offline. The testing stage of the proposed SVM-based method is very fast and therefore can be used in real-time.

Acknowledgement

We would like to thank Drs. Emad Boctor, Michael Choti and Gregory Hager from Johns Hopkins University for sharing the data with us.

REFERENCES

[1] M. Ghasemi Amidabadi, M. Omair Ahmad, and H. Rivaz, "Supervised classification of the accuracy of the time delay estimation in ultrasound elastography," *IEEE Trans. Ultrasonics Ferroelectrics Frequency Control (TUFFC)*, Accepted.

[2] J. Ophir, I. Cespedes, H. Ponnekanti, Y. Yazdi, and X. Li, "Elastography: a quantitative method for imaging the elasticity of biological tissues," *Ultrasonic Imaging*, vol. 13, no. 2, pp. 111–134, 1991.

[3] G. Treece, J. Lindop, L. Chen, J. Housden, R. Prager, and A. Gee, "Real-time quasi-static ultrasound elastography," *Interface Focus*, vol. 1, no. 4, pp. 540–552, 2011.

[4] M. O'Donnell, A. R. Skovoroda, B. M. Shapo, S. Y. Emelianov *et al.*, "Internal displacement and strain imaging using ultrasonic speckle tracking," *IEEE Transactions on Ultrasonics Ferroelectrics and Frequency Control*, vol. 41, no. 3, pp. 314–325, 1994.

[5] A. Kuzmin, A. M. Zakrzewski, B. W. Anthony, and V. Lempitsky, "Multi-frame elastography using a handheld force-controlled ultrasound probe," *IEEE Transactions on Ultrasonics, Ferroelectrics, and Frequency Control*, vol. 62, no. 8, pp. 1486–1500, 2015.

[6] G. C. Carter, *Coherence and time delay estimation: an applied tutorial for research, development, test, and evaluation engineers*. IEEE, 1993.

[7] W. F. Walker and G. E. Trahey, "A fundamental limit on delay estimation using partially correlated speckle signals," *IEEE Transactions on Ultrasonics, Ferroelectrics, and Frequency Control*, vol. 42, no. 2, pp. 301–308, 1995.

[8] A. Weiss and E. Weinstein, "Fundamental limitations in passive time delay estimation–part i: Narrow-band systems," *IEEE Transactions on Acoustics, Speech, and Signal Processing*, vol. 31, no. 2, pp. 472–486, 1983.

[9] I. Cespedes, M. Insana, and J. Ophir, "Theoretical bounds on strain estimation in elastography," *IEEE Transactions on Ultrasonics, Ferroelectrics, and Frequency Control*, vol. 42, no. 5, pp. 969–972, 1995.

[10] T. Varghese and J. Ophir, "A theoretical framework for performance characterization of elastography: The strain filter," *IEEE Transactions on Ultrasonics, Ferroelectrics, and Frequency Control*, vol. 44, no. 1, pp. 164–172, 1997.

[11] Y.-C. Chang, M.-C. Yang, C.-S. Huang, S.-C. Chang, G.-Y. Huang, W. K. Moon, and R.-F. Chang, "Automatic selection of representative slice from cine-loops of real-time sonoelastography for classifying solid breast masses," *Ultrasound in Medicine & Biology*, vol. 37, no. 5, pp. 709–718, 2011.

[12] S.-C. Chang, Y.-W. Lee, Y.-C. Lai, C.-M. Tiu, H.-K. Wang, H.-J. Chiou, Y.-W. Hsu, Y.-H. Chou, and R.-F. Chang, "Automatic slice selection and diagnosis of breast strain elastography," *Medical Physics*, vol. 41, no. 10, p. 102902, 2014.

[13] E. Shaswary, Y. Xu, and J. Tavakkoli, "Performance study of a new time-delay estimation algorithm in ultrasonic echo signals and ultrasound elastography," *Ultrasonics*, vol. 69, pp. 11–18, 2016.

[14] R. Xia, G. Tao, and A. K. Thittai, "Dynamic frame pairing in real-time freehand elastography," *IEEE Transactions on Ultrasonics, Ferroelectrics, and Frequency Control*, vol. 61, no. 6, pp. 979–985, 2014.

[15] A. Gee, J. Lindop, G. Treece, R. Prager, and S. Freeman, "Stable, intelligible ultrasonic strain imaging," *Ultrasound*, vol. 16, no. 4, pp. 187–192, 2008.

[16] G. M. Treece, J. E. Lindop, A. H. Gee, and R. W. Prager, "Uniform precision ultrasound strain imaging," *IEEE Transactions on Ultrasonics, Ferroelectrics, and Frequency Control*, vol. 56, no. 11, pp. 2420–2436, 2009.

[17] J. E. Lindop, G. M. Treece, A. H. Gee, and R. W. Prager, "An intelligent interface for freehand strain imaging," *Ultrasound in Medicine & Biology*, vol. 34, no. 7, pp. 1117–1128, 2008.

[18] H. Khodadadi, A. G. Aghdam, and H. Rivaz, "Edge-preserving ultrasonic strain imaging with uniform precision," in *Proc. 37th IEEE International Conference on Engineering, Medicine and Biology (EMBC)*, 2015, pp. 3835–3838.

[19] J. Jiang, T. J. Hall, and A. M. Sommer, "A novel performance descriptor for ultrasonic strain imaging: a preliminary study," *IEEE Transactions on Ultrasonics, Ferroelectrics, and Frequency Control*, vol. 53, no. 6, pp. 1088–1102, 2006.

[20] B. R. Chintada, A. V. Subramani, B. Raghavan, and A. K. Thittai, "A novel elastographic frame quality indicator and its use in automatic representative-frame selection from a cine loop," *Ultrasound in Medicine & Biology*, 2016.

[21] H. Rivaz, E. M. Boctor, M. A. Choti, and G. D. Hager, "Real-time regularized ultrasound elastography," *IEEE Transactions on Medical Imaging*, vol. 30, no. 4, pp. 928–945, 2011.

[22] H. S. Hashemi and H. Rivaz, "Global time-delay estimation in ultrasound elastography," *IEEE Transactions on Ultrasonics, Ferroelectrics, and Frequency Control*, vol. 64, no. 10, pp. 1625–1636, 2017.